Mass Action Modeling of Catalysis Through Reaction Flux Estimation

Author: Ethan Stancliffe, Biomedical Engineering and Mathematics

Faculty Mentor: Dr. Michael Mackey, Department of Biomedical Engineering

Honors Advisor: Dr. David Wilder, Department of Biomedical Engineering

Abstract

The complexity of biochemical networks necessitates the use of computational and mathematical frameworks to accurately characterize and study these systems. However, modern frameworks developed for this task have inadequacies that limit their accuracy or scalability. In this report, a mathematical model of the canonical enzyme substrate binding network is developed, and, using estimated true and maximal reaction rates, a methodology utilizing principles of flux balance analysis is developed to deduce the individual reaction rate constants in the network. It is then shown that these two reaction rates are not sufficient to unambiguously define a mass action kinetic model of this network. Nevertheless, the methodology developed greatly reduces the degrees of freedom of the system, and, as a result, the solution space of the network can be examined computationally and analytically revealing several non-intuitive sensitivities.

Introduction

Biochemical networks have long fascinated biophysicists and, recently, systems biologists. The biological networks that govern cellular decision making, metabolism, etc. are often complex and highly nonlinear; as such, there is a need to study and model these networks *in silico* to systematically compile biological information and predict the often non-intuitive behavior of these networks under a multitude of environmental and structural conditions. In so doing, the time and expense required by traditional biochemical experimentation to characterize these networks can be reduced, and, further, the elucidation of unobservable or immeasurable phenomena will be possible.

One approach to modeling metabolic networks has been bolstered through the development of flux balance analysis or FBA (Gianchandani, Chavali, & Papin, 2010). This computational tool utilizes linear programming and steady state conservation relations to find optimal reaction rates, or fluxes, for each reaction within the metabolic model. A stoichiometric matrix, *S*, is created that encapsulates the stoichiometry of each reaction. In this matrix, each column represents a reaction and each row a chemical species. With this matrix, conservation of mass can be employed such that, at steady state, the following relation exists, where v is a vector containing the flux value for each reaction.

$$S \cdot v = 0 \quad (1)$$

Unfortunately, for most networks, this system is underdetermined and before the analysis can be completed, an objective function must be formulated such that linear programming can find an optimal solution. This objective function generally consists of a single reaction containing a multitude of chemical species that are thought to represent a biomass-forming reaction (Feist & Palsson, 2010). Thus, the linear program searches the solution space for the largest flux value of the biomass forming reaction thereby optimizing the system for growth (Gianchandani et al., 2010).

The power of these models lie in their ability to produce quantitative predictions without the necessity for knowing biophysical constants that are necessary to parametrize alternative modeling approaches, such as an ordinary differential equations (ODE) based mass action model. Flux balance analysis allows for the behavior of a system to be estimated under well-defined perturbations. For example, in genome scale metabolic modeling, metabolic genes are identified and linked together with logical AND/OR relationships that connect to a reaction (Haggart, Bartell, Saucerman, & Papin, 2011). From these relationships it is then possible to determine the behavior of the network when a gene is inactivated *in silico* by examining the predicted biomass

reaction flux and pathway utilizations (Haggart et al., 2011). The perturbations that can be explored with these models are discreet by nature. For example, decreased enzyme affinity or increased competition cannot be simulated using these models. The components are binary: on or off, and although they allow for a reduction in computational expense and negate the need for explicit rate constant definition, subtle perturbation simulations cannot be achieved. Ideally, these models could be enhanced through the addition of kinetics.

The principle of mass action asserts that under infinitely well stirred, isothermal, conditions the rate of a reaction is proportional to the concentrations of the reactants raised to their respective stoichiometric powers, shown in Figure 1. This assertion allows for an ODE model to be constructed to capture the nonlinear complexity of biological networks. However, to make such a model functional, rate constants need to be determined for each elementary reaction within the network.

$$xA + yB \xrightarrow{k} F$$

$$\frac{dC_F}{dt} = kC_A^x C_B^y$$

Figure 1: The principle of mass action states that the rate of an elementary reaction is the product of a rate constant, k, and the concentration of the reactants, A and B raised to their respective stoichiometric coefficients, x and y (Érdi, 1989).

These biophysical constants are often difficult to measure experimentally or predict theoretically. Although it is possible to deduce these values through modern structural protein modeling and simulation, the computation time is still too large to deduce the constants required for large scale biochemical modeling (Gräter & Li, 2015). Experimentally, Michaelis-Menten analysis (Goudar, Sonnad, & Duggleby, 1999) has been used to deduce approximate values of rate constants through measuring the rate of an enzymatic reaction as a function of substrate concentration. However, many of the assumptions employed in the formal derivation of the Michaelis Equation (Michaelis, Menten, Johnson, & Goody, 2011) are not valid under

physiological conditions (Schnell, 2014), (Grima & Schnell, 2006), (Zhou, Rivas, & Minton, 2008). Additionally, this analysis does not produce all of the constants needed to parametrize a mass action kinetic model. Ideally, the lumped reaction rate, found through applying flux balance analysis to a biochemical network, and an experimentally estimated maximal rate would provide sufficient constraint to deduce closed form solutions for the rate constants of a mass action mathematical model. This would allow for the kinetics of the network to be studied without a significant increase in modeling complexity.

However, before a mass action parametrization paradigm could be implemented within an entire genome scale metabolic model, the validity of this approach must be shown for a simple network. This investigation studies the canonical enzyme substrate binding model that is utilized in Michaelis-Menten analysis (Michaelis et al., 2011), shown in Figure 2. Although this biochemical network is simple, its vast use in enzymatic study provides the motivation for its examination.

Figure 2: Simple reaction network utilized in Michaelis-Menten Analysis representing uninhibited enzyme substrate binding.

In this report, a mathematical model of this network is created, and, using estimated true and maximal reaction rates, a method utilizing principles of flux balance analysis is developed to deduce the individual reaction rate constants in the network. In the Methodology, this method is mathematically derived and rigorously examined for a general case. Following, the Results and Discussion section apply this methodology with a specific true and maximal reaction rate to create a constrained mass action kinetic model. This model is then examined analytically and

computationally to expose the non-intuitive behavior and sensitivities of this network. Finally, in the Conclusion, an experimental protocol will be proposed to calculate the values of these rate constants.

Methodology

Development of the Biochemical Test Network

To test the validity of defining a mass action biochemical model of a simple reaction network from a lumped reaction rate and a maximal rate, the enzyme substrate binding model shown in Figure 3 was used. In this network, substrate enters the system continuously at a fixed rate V_{in} and product flows out of the system at the lumped reaction rate, V_{out}, during steady state. The enzyme, E, and substrate, S, combine to form the intermediate complex, ES, where the product, P, is produced and the enzyme is released. For this system it is assumed that the substrate concentration remains constant throughout the simulation as substrate in pumped into the system at the same rate at which it is consumed.

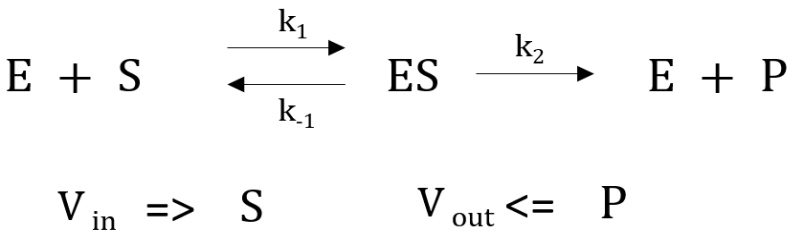

Figure 3: Reaction network under investigation. This network involves uninhibited enzyme substrate binding with the substrate flowing into the network at a constant rate V_{in} and product diffusing out in proportion to product concentration eventually leading to a steady state rate of *Vout*. Each elementary reaction in this network is given a rate constant k_i, which is unknown.

Mathematical Modeling

Using the principle of mass action (Érdi, 1989), a mathematical model of this network was constructed and is shown below. However, for this model to be functional, closed form solutions for the rate constants, k_1, k_2, and k_3, need to be derived from the elementary steady state reaction rates of the network and initial conditions. For completeness, a fourth rate constant, k_0, must be defined to represent the coefficient of product diffusion. However, since the

concentration of product does not appear in any term of equation (2) that relates to enzyme, substrate, or enzyme-substrate complex concentrations, the product concentration is trivial for this analysis, as such, for simplicity $k_0 = 1$.

$$\begin{aligned}
\frac{dC_E(t)}{dt} &= -k_1 C_E(t) C_S(t) + k_{-1} C_{ES}(t) + k_2 C_{ES}(\mathrm{t}) \\
\frac{dC_S(t)}{dt} &= -k_1 C_E(t) C_S(t) + k_{-1} C_{ES}(t) + V_{in} \\
\frac{dC_{ES}(t)}{dt} &= k_1 C_E(t) C_S(t) - k_{-1} C_{ES}(t) - k_2 C_{ES}(t) \\
\frac{dC_P(t)}{dt} &= k_2 C_{ES}(t) - k_0 C_P(t)
\end{aligned} \tag{2}$$

To find the steady state reaction rates for each elementary step in the network, FBA can be employed to systematically deduce these values. To form the linear program, it is necessary to develop a stoichiometric S matrix shown below in equation (3).

$$\begin{array}{cccccc}
S\,Matrix: & E + S \rightarrow ES & ES \rightarrow E + S & ES \rightarrow E + P & \rightarrow S & P \rightarrow \\
E & -1 & 1 & 1 & 0 & 0 \\
S & -1 & 1 & 0 & 1 & 0 \\
ES & 1 & -1 & -1 & 0 & 0 \\
P & 0 & 0 & 1 & 0 & -1
\end{array} \tag{3}$$

Additionally, the domain of flux values must be established. As discussed above, for this network, the rate of product removal at steady state is V_{out}, and the maximal possible rate (the rate if the reversibility of the enzyme-substrate complex formation is 0, $k_{-1} = 0$) is V_{max}. Following, the domain of the flux vector is given in equation (4).

$$Z = \begin{bmatrix} [0, \infty) \\ V_{max} - V_{out} \\ [0, \infty) \\ [0, \infty) \\ V_{out} \end{bmatrix} \tag{4}$$

Before the linear program is fully developed, the final requirement is that an objective function be defined. However, for this network, this step is trivial, in that regardless of the choice of reaction flux to maximize, only a singular solution can exist to equation (1). However, for completeness, an objective vector, *C*, will be defined, where the defined steady state removal of product is to be maximized.

$$C = \begin{bmatrix} 0 \\ 0 \\ 0 \\ 0 \\ 1 \end{bmatrix} \tag{5}$$

With the above definitions, the following linear program is formulated.

$$\max(v \cdot c) \ \ subject\ to \tag{6}$$

$$v \ \in Z$$

$$S \cdot v = 0$$

Which, upon solving, reaction rates (fluxes) for each elementary step within the network are unambiguously defined. These flux values can be related to the rate constants that exist within the mass action model by solving equation (2) for a time $t = \beta$, where β is some time at which the rate of formation of each species, *i*, in the network is 0 or, equivalently, the system is at steady state.

$$v_f = \begin{bmatrix} v_1 \\ v_2 \\ v_3 \\ v_4 \\ v_5 \end{bmatrix} = \begin{bmatrix} V_{max} \\ V_{max} - V_{out} \\ V_{out} \\ V_{out} \\ V_{out} \end{bmatrix} = \begin{bmatrix} k_1 C_E(\beta) C_S(\beta) \\ k_{-1} C_{ES}(\beta) \\ k_2 C_{ES}(\beta) \\ V_{in} \\ k_0 C_P(\beta) \end{bmatrix} = \begin{bmatrix} k_1 C_E(\beta) C_S(\beta) \\ k_{-1} C_{ES}(\beta) \\ k_2 C_{ES}(\beta) \\ V_{in} \\ C_P(\beta) \end{bmatrix} \tag{7}$$

However, this relationship is insufficient to determine the rate constant values, k_i. Additionally, the relations given in equation (2) do not determine a definitive relationship of k_i to

the flux vector, v_f. Evaluating equation (2) when $t = \beta$, yields the following relation for $\frac{dC_E(t)}{dt}$.

$$\frac{dC_E(\beta)}{dt} = 0 = k_1 C_E(\beta) C_S(\beta) + k_{-1} C_{ES}(\beta) + k_2 C_{ES}(\beta) = -v_1 + v_2 + v_3 \quad (8)$$

Using equations (7) and (8), the system can be compacted into matrix form and reduced using Gaussian Elimination. Following reduction, the system returns to the relation given in equation (7) and is still underdetermined.

$$\begin{bmatrix} C_E(\beta)C_S(\beta) & 0 & 0 \\ 0 & C_{ES}(\beta) & 0 \\ 0 & 0 & C_{ES}(\beta) \\ C_E(\beta)C_S(\beta) & -C_{ES}(\beta) & -C_{ES}(\beta) \end{bmatrix} \begin{bmatrix} k_1 \\ k_{-1} \\ k_2 \end{bmatrix} = \begin{bmatrix} v_1 \\ v_2 \\ v_3 \\ 0 \end{bmatrix} \quad (9)$$

$$= \begin{bmatrix} C_E(\beta)C_S(\beta) & 0 & 0 \\ 0 & C_{ES}(\beta) & 0 \\ 0 & 0 & C_{ES}(\beta) \\ 0 & 0 & 0 \end{bmatrix} \begin{bmatrix} k_1 \\ k_{-1} \\ k_2 \end{bmatrix} = \begin{bmatrix} v_1 \\ v_2 \\ v_3 \\ -v_1 + v_2 + v_3 \end{bmatrix} = \begin{bmatrix} v_1 \\ v_2 \\ v_3 \\ 0 \end{bmatrix}$$

$$\rightarrow \begin{bmatrix} C_E(\beta)C_S(\beta) & 0 & 0 \\ 0 & C_{ES}(\beta) & 0 \\ 0 & 0 & C_{ES}(\beta) \end{bmatrix} \begin{bmatrix} k_1 \\ k_{-1} \\ k_2 \end{bmatrix} = \begin{bmatrix} v_1 \\ v_2 \\ v_3 \end{bmatrix}$$

Constraining the System

To further constrain the system, two assumptions can be implemented. The first being that since the substrate concentration is much greater than the initial enzyme concentration, and substrate is being pumped into the system at exactly the same rate at which it is consumed at steady state, the concentration of substrate does not vary with time: $\frac{dC_S(t)}{dt} = 0$, and thus, $C_S(t) = C_S(0) = S_0$. Secondly, if enzyme cannot be transported across the system boundary, there is a conservation.

$$C_E(0) = C_E(t) + C_{ES}(t) = E_0 \quad (10)$$

These two assumptions can be implemented into equation (9), yielding equation (11).

$$\begin{bmatrix} C_E(\beta)\mathrm{C_S}(\beta) & 0 & 0 \\ 0 & C_{ES}(\beta) & 0 \\ 0 & 0 & C_{ES}(\beta) \end{bmatrix} \begin{bmatrix} k_1 \\ k_{-1} \\ k_2 \end{bmatrix} = \begin{bmatrix} v_1 \\ v_2 \\ v_3 \end{bmatrix} = \begin{bmatrix} (E_0 - C_{ES}(\beta) * \mathrm{S_0} & 0 & 0 \\ 0 & C_{ES}(\beta) & 0 \\ 0 & 0 & C_{ES}(\beta) \end{bmatrix} \begin{bmatrix} k_1 \\ k_{-1} \\ k_2 \end{bmatrix} \quad (11)$$

Computational Analysis

This system, although still underdetermined, now exists with only one free variable. As such, the solution space and sensitivities can be reasonably explored computationally. The mass action model, equation (2), was implemented within a python script using the Numerical Python (van Der Walt et al., 2011) and Scientific Python (Jones, Oliphant, Peterson, & al., 2001) packages. The dynamics of this model were sampled by defining a value for each rate constant independently, following, the model was then parametrized by using equation (11). Following parameterization, the system was simulated using the odeint numerical differential equation solver for 700 time steps.

Each rate constant was systematically sampled with *n = 1000* in a domain spanning four orders of magnitude, in correspondence with the domain of each rate constant. This domain was found from equation (11) and the conservation of enzyme which requires that $C_{ES}(\beta) \in [0, E_0]$. These two relations form the below inequalities, equation (12), which serve as lower bounds for the rate constants values. The sampling interval was then designed with the lower bounds found from equation (12) and the upper bounds being four orders of magnitude greater.

$$\frac{v_1}{S_0 E_0} \leq k_1 \qquad \frac{v_2}{E_0} \leq k_{-1} \qquad \frac{v_3}{E_0} \leq k_2 \quad (12)$$

Further, the stability of the network can be examined. From equation (11), the only variable that is not a rate constant is the steady state complex concentration, $C_{ES}(\beta)$. As such, $C_{ES}(\beta)$ can be solved for in terms of each rate constant independently, yielding equation (13).

$$C_{ES}(\beta) \;=\; E_0 - \frac{v_1}{k_1 S_0} = \frac{v_2}{k_{-1}} = \frac{\mathrm{v_3}}{\mathrm{k_2}} \tag{13}$$

Then, the first derivative of $C_{ES}(\beta)$ with respect to each rate constant can be found yielding equations (14-16).

$$\frac{dC_{ES}(\beta)}{dk_1} = \; -\frac{v_1}{S_0 k_1^2} \tag{14}$$

$$\frac{dC_{ES}(\beta)}{dk_{-1}} = \; -\frac{v_2}{k_{-1}^2} \tag{15}$$

$$\frac{dC_{ES}(\beta)}{dk_2} = \; -\frac{v_3}{k_2^2} \tag{16}$$

This relation, along with the lower rate constant bound found from equation(12), allows for the maximal sensitivity with respect to each rate constant to be calculated, yielding equations (17-19).

$$\max\left(\left|\frac{dC_{ES}(\beta)}{dk_1}\right|\right) = \; \frac{S_0 E_0^2}{v_1} \tag{17}$$

$$\max\left(\left|\frac{dC_{ES}(\beta)}{dk_{-1}}\right|\right) = \; \frac{E_0^2}{v_2} \tag{18}$$

$$\max\left(\left|\frac{dC_{ES}(\beta)}{dk_2}\right|\right) = \; \frac{E_0^2}{v_3} \tag{19}$$

Additionally, it can be shown that $\lim_{k_i \to \infty} \left|\frac{dC_{ES}(\beta)}{dk_i}\right| = 0 \;\; for\ all\ i \in \{1, -1, 2\}$, therefore $C_{ES}(\beta)$ is asymptotically stable. To determine the dynamics of the near-stable regions of the system, k_1 and k_{-1} were chosen independently such that $\left|\frac{dC_{ES}(\beta)}{dk_i}\right| \leq$ .0001. Using (11) and (14-15), the following inequalities are established for the rate constants in a near stable region, (20-21).

$$k_1 \;\geq \sqrt{\frac{v_1}{(.0001) S_0}} \tag{20}$$

$$k_{-1} \geq \sqrt{\frac{v_2}{.0001}} \tag{21}$$

The minimally stable systems were then parameterized by deducing all other rate constant values using (11) and computationally simulated using the numerical ODE solver mentioned above.

Results and Discussion

After rigorous mathematical analysis of the enzyme substrate binding model discussed above, it was shown that the deduced elementary reaction rates were not sufficient to define the rate constants embedded within the mass action kinetic model. However, after implementing many of the assumptions utilized in Michaelis Menten analysis, the system was reduced to a single free variable. To computationally examine the solution space of the model, an arbitrary product diffusion flux, V_{out}, was defined to be 13 and the maximal flux, V_{max}, was defined to be 15. Additionally, initial conditions were given with an initial substrate concentration, S_0, of 1000 and enzyme concentration, E_0, of 5, with the value of k_0 again being 1. For all other species, initial concentrations were set to 0. For this analysis, units are trivial. However, in practice flux values are often given in *moles/second* and concentration in *moles*. From (7), with V_{out}, = 13 and $V_{max} = 15$, the following flux vector was produced.

$$v_f = \begin{bmatrix} v_1 \\ v_2 \\ v_3 \\ v_4 \\ v_5 \end{bmatrix} = \begin{bmatrix} V_{max} \\ V_{max} - V_{out} \\ V_{out} \\ V_{out} \\ V_{out} \end{bmatrix} = \begin{bmatrix} 15 \\ 2 \\ 13 \\ 13 \\ 13 \end{bmatrix} = \begin{bmatrix} k_1 C_E(\beta) C_S(\beta) \\ k_{-1} C_{ES}(\beta) \\ k_2 C_{ES}(\beta) \\ V_{in} \\ k_0 C_P(\beta) \end{bmatrix} = \begin{bmatrix} k_1(5 - C_{ES}(\beta))(1000) \\ k_{-1} C_{ES}(\beta) \\ k_2 C_{ES}(\beta) \\ V_{in} \\ C_P(\beta) \end{bmatrix} \quad (22)$$

To examine the solution space of this system, each rate constant was sampled individually, and the system was simulated for 1000 time steps. In the case of the first rate constant, k_1, near singular dynamics were observed from the network with only slight variations in substrate concentrations occurring. However, since substrate concentration was assumed constant throughout the simulation, the dynamics of the network can be considered identical. Additionally, final steady state concentrations of free enzyme were near zero for all sampled values of k_1. As such, nearly all the enzyme in the system was in the bound complex state. However, in examining the behavior of the system at values of k_1 near the lower bound, found

from (12), there was an increase in sensitivity with steady state enzyme concentrations varying rapidly as the value of k_1 changes.

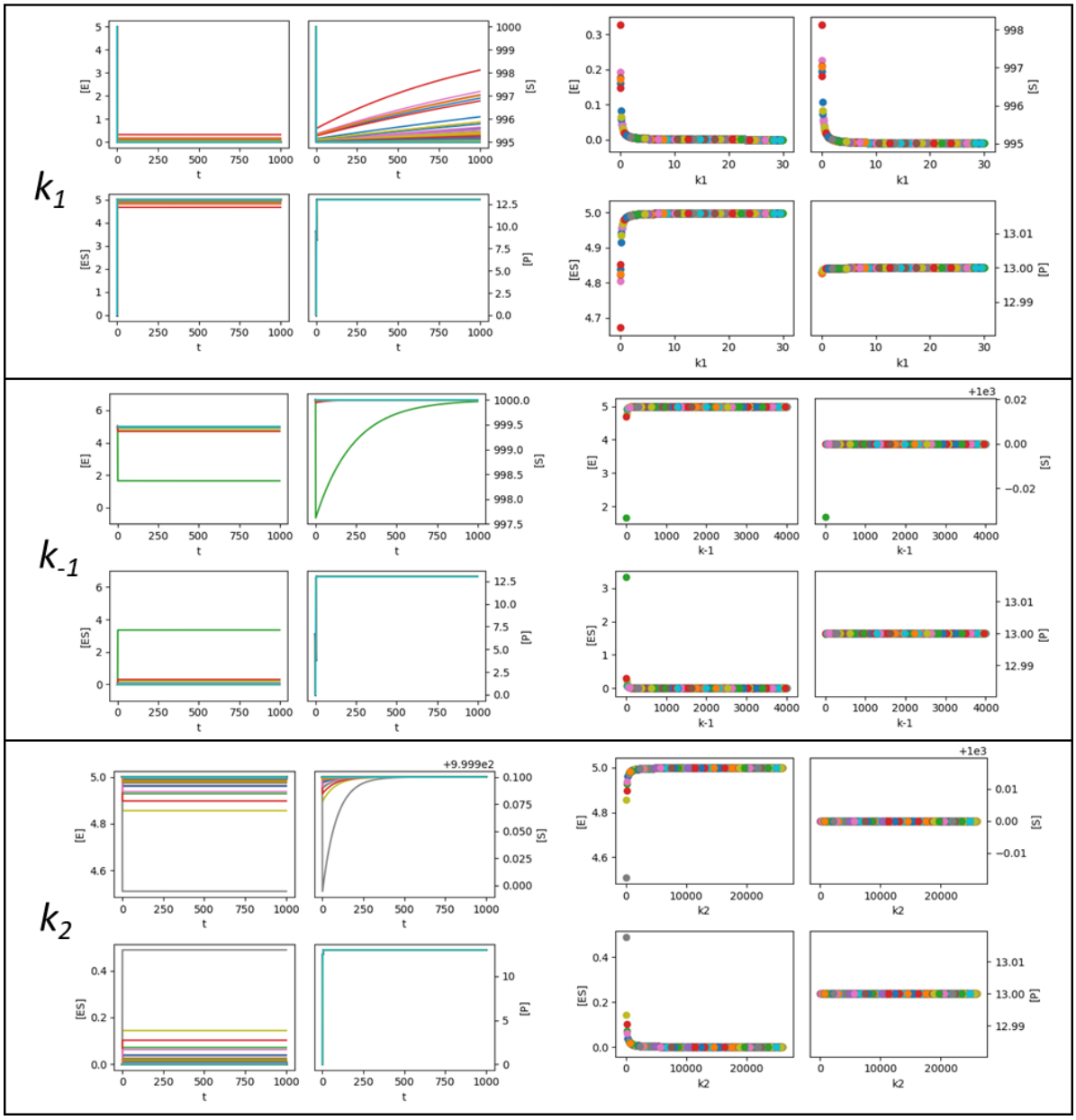

Figure 3: Enzyme substrate binding kinetics under rate constant sampling. Each rate constant, k_1, k_{-1}, k_2, was independently sampled from a domain spanning nine orders of magnitude for k_1 and three for k_{-1} and k_2. An increase in sensitivity was observed as rate constant values approach zero. Additionally, a greater dynamic range was produced over the sampling of k_{-1} and k_2.

In the case of k_{-1}, at large rate constant values free enzyme concentration approached zero, while the enzyme substrate complex concentrations approached five. This dynamic

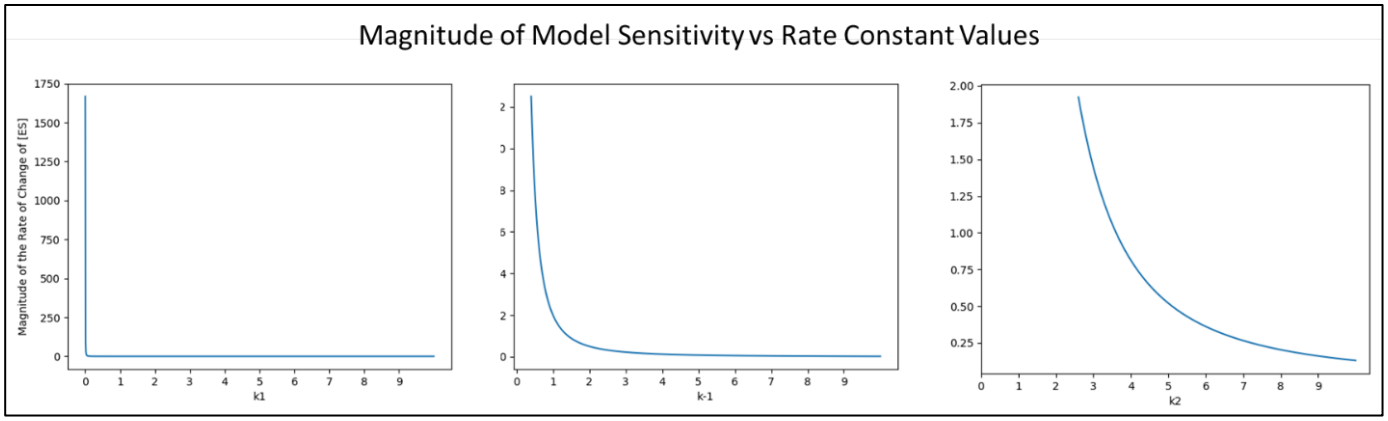

Figure 4: The magnitude of the first derivative of the of the steady state substrate enzyme complex with respect to each rate constant is plotted above as a function of said rate constant. In each case the greatest sensitivity was observed at the lower rate constant bound and asymptotically approaches 0 as it increased

signature is the opposite as what was seen when k_1 was sampled at large values. In keeping with the behavior seen in the previous exploration, there again was enhanced parameter sensitivity at k_{-1} values near the lower bound. At low values, steady state enzyme concentrations decreased rapidly, approaching the dynamic signature observed at high values of k_1. Similarly, in sampling k_2 at large values, an identical dynamic signature as that produced at large, k_{-1} was observed. However, the value at which the increased sensitivity began was greater than in the previous examination.

In all explorations, there existed sensitivity at rate constant values near the lower bound of their respective domain, and, further, the result of this sensitivity was instability in the steady state concentrations of the enzyme complex, as $C_{ES}(\beta)$ varied smoothly in the interval $(0, E_0)$, shown in Figure 4. To examine this sensitivity in greater detail, equations (14-16) can be evaluated at rate constant values near their respective lower bounds. From this comparison, the maximal model sensitivity occurred with values of k_1 near its lower bound of 0.003, and the sensitivity asymptotically went zero with increasing rate constant values. Similarly, in k_{-1} and k_2, the maximal sensitivity occurred at the lower bound of the rate constant values, 0.4 and 2.6

respectively. However, the maximal rate of change in the steady state concentration of enzyme complex with respect to the rate constants, k_{-1} and $k_{2,}$ was approximately three orders of magnitude less than that with respect to k_1, and the stability of k_1 increased as k_1 increased in value and did so more rapidly that the other two rate constants which underwent a more gradual transition into instability.

To fully describe the stable regions of this network, the dynamics were examined with rate constant values defined first for k_1 and then for k_{-1}. This was sufficient as k_{-1} and k_2 differ only by a scaling factor, as shown above in equation (14) and in Figure 5. Following the analysis, the same stable dynamics were observed for a stable k_{-1} as for a stable k_2. To observe these stable dynamics, minimal rate constant values were chosen from the range given in equations (20-21), yielding the following two sets of rate constant parameters from equation (11):

$\{k_1, k_{-1}, k_2\} = \{12.24, 0.40009, 2.6006\}$,

$\{0.003008, 141.4, 919.1\}$.

These two parameter sets, describe the two, distinct, stable dynamical signatures, shown in Figure 6, which can be produced

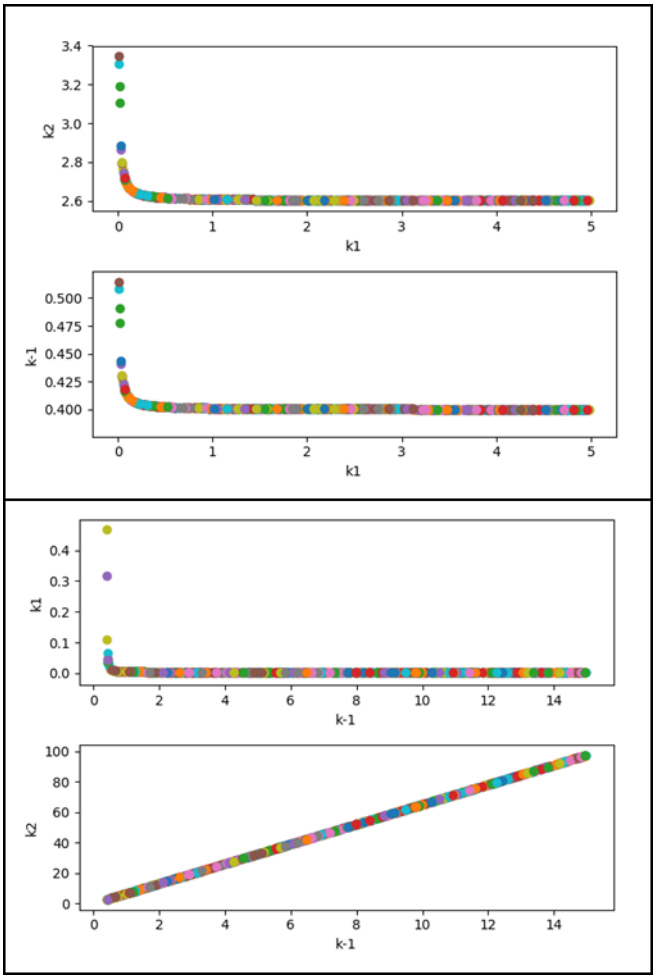

Figure 5: Rate constants, k_1, k_{-1}, k_2, as a function of k_1 *and* k_{-1}. It is unnecessary to examine the rate constants as function of k_2 as they only differ from k_{-1} by a scale factor.

from this network. In the first, for large values of k_1, k_{-1} and k_2 remain near their respective lower bound. As such, free enzyme concentrations were near zero at steady state, with bound complex concentrations near E_0. In the second parameter set, k_{-1} and k_2 were large and k_1 was near its lower bound. Consequently, the opposite dynamics were observed: bound complex concentrations were near zero and free enzyme concentrations were near E_0. Therefore, it was concluded that when the steady state concentration of enzyme was on the order of the

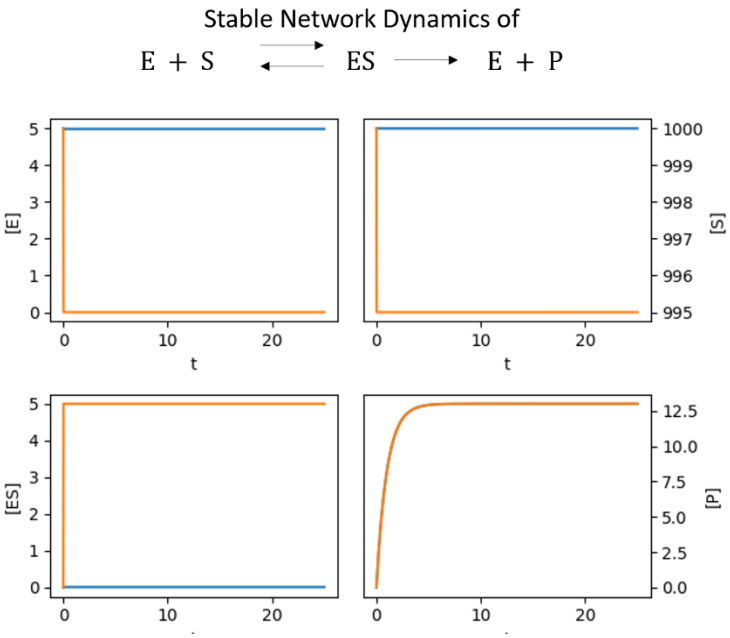

Figure 6: Stable dynamics of the enzyme substrate binding network under investigation. The orange curves represent the solution of (2) with {*k1, k-1, k2*} = {12.24, 0.40009, 2.6006} and the blue curves with {*k1, k-1, k2*} = {0.003008, 141.4, 919.1}.

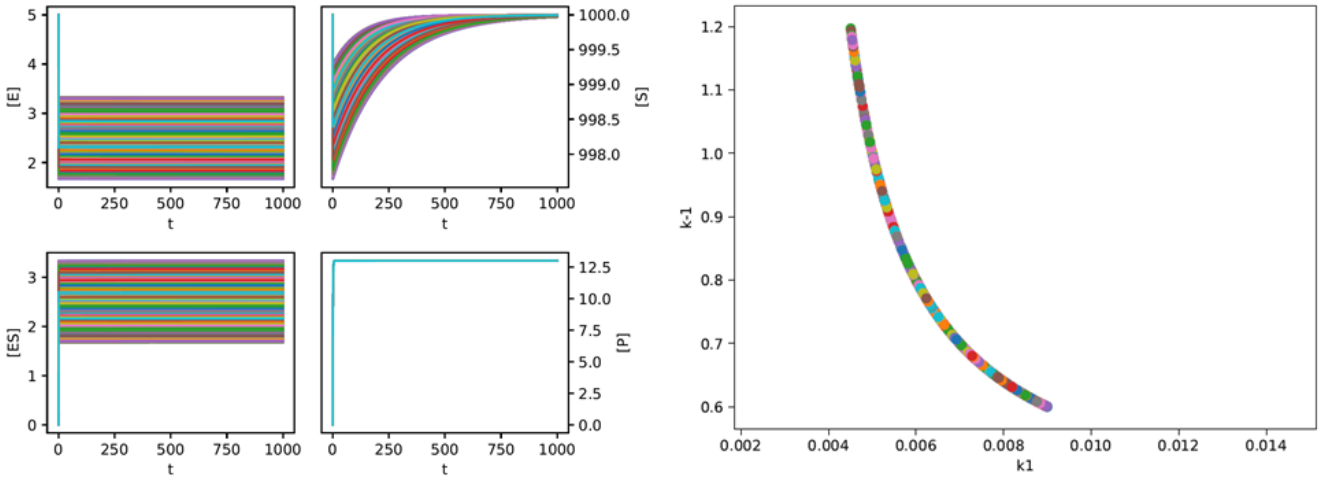

Figure 7: Left: System dynamics when k_1 was sampled in a domain, [0.0045, 0.009], which generated steady state free and complexed enzyme concentrations intermediate to the dynamic signatures of the stable rate constant sets. Right: The relationship between k_1 and k_{-1} is shown. In this domain, a more linear relationship existed between the rate constants then in the stable dynamics. The relationship between k_1 and k_2 was the same as that for k_1 and k_{-1}, with the only difference being a scale factor formed from the ratio of v_3/v_2.

steady state concentration of enzyme substrate complex, instability existed in the system where a small perturbation in rate constant values resulted in large variations in steady state chemical concentrations. Consequently, this scenario also resulted in a more linear relationship between k_1 and the other two rate constants.

In this context, biochemical network regulation factors into the interpretation and significance of the sensitivities and stable dynamics of the system. Rate constants can be considered to represent the activity of the enzyme, and although for most globular enzymes it is reasonable to assume their value will remain constant throughout a binding reaction (Érdi, 1989), they are dependent on external factors (temperature, pH, etc.) and structural considerations that alter their activity. The sensitivities that existed in the two stable dynamic states represent the aspects of the network with high potential for regulation. When steady state free enzyme concentration was near E_0, the system was very sensitive to k_1. Conversely, when enzyme complex concentration was near E_0, the system was highly sensitive to both k_{-1} and k_2. Making use of the dependence between k_{-1} and k_2, complete regulation of the system was possible

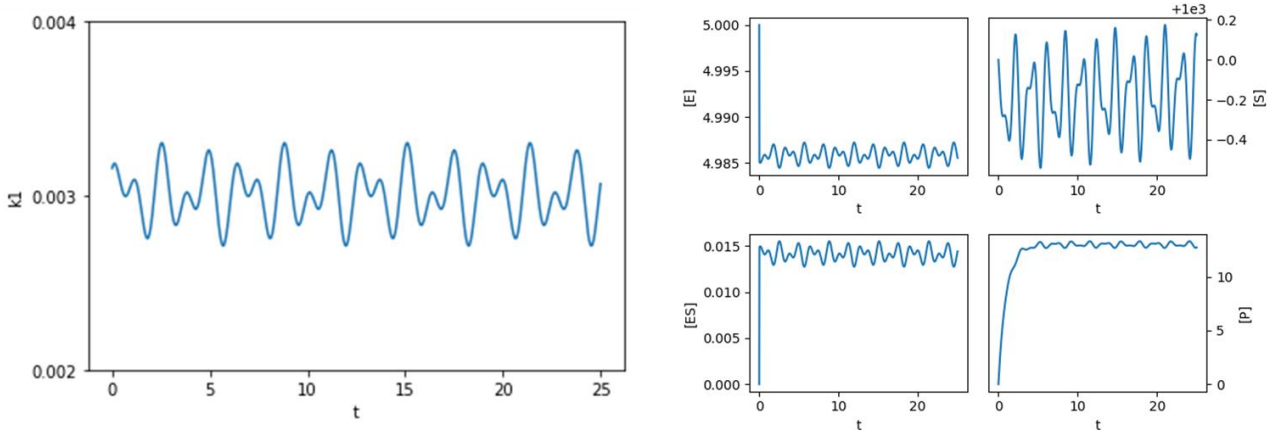

Figure 8: Network dynamics at the steady dynamic signature produced when $\{k_1, k_{-1}, k_2\} = \{0.003008, 141.4, 919.1\}$, but k_1 oscillates: $k_1(t) = (0.003008) + (0.003008)(.05)(\sin(3t) + \cos(5t))$, shown on the left. The perturbation translates through the network producing the more complex dynamics seen on the right.

through k_{-1} and k_1, which both belong to the preliminary binding reaction, E + S ⇋ ES. This reaction is then an ideal target to regulate the dynamics of this network.

The stability of the two opposite dynamical states were also suggestive of a biological switch. The network could easily transition between the two stable states, because at no dynamic state was the network insensitive to any rate constant. Through fine regulation of the enzyme activity, more complex time varying dynamics could be produced from this network simply through an oscillating temperature. To show this phenomenon, in the stable state defined by $\{k_1, k_{-1}, k_2\} = \{0.003008, 141.4, 919.1\}$, when k_1 oscillated within 5% of its value, after simulation the perturbed rate constant translated its value through the network due to the sensitivity.

Although complete parameterization of this network was not possible through definition of the lumped reaction rate and maximal rate, it did allow for rigorous mathematical analysis of the system at steady state. From this study, insight into the sensitivities of this network were obtained that allowed for determination of stable dynamic signatures that are unique to this network. In this section, a single set of reaction flux values were used in the analysis, but this approach generalizes nicely as shown in the Methodology.

Conclusion

This study, while limited in scope, demonstrates the complexity that exists in even the simplest of biological networks. Further, by elucidating the range of dynamics that can be obtained from such a system, the importance of rigorous modeling is amplified. Modern techniques developed for metabolic modeling, such as flux balance analysis, ignore these complexities, and although they allows for specific quantitative predictions, the large ambiguity that exists in these models must be recognized and treated appropriately. It may be that modeling frameworks that do not require kinetic information are incapable of predicting chemical concentrations and the mechanisms of regulation that exist in many such biological networks.

In addition to exposing the ambiguities in modern modeling frameworks, this study also provides a framework to experimentally derive the value of these rate constants. The mathematics developed in this study required that the rates of true and maximal (if no reversibility is assumed) product formation be known. An estimate of the latter can be easily achieved in a laboratory setting by placing a known quantity of substrate into a well-mixed solution, containing the enzyme, and measuring the quantity of product produced. If no reversibility existed in the network, obviously the amount of product formed should equal the amount of substrate. The ratio of substrate input, S_{in}, and product production, v_{actual}, then can be used as a scale factor to estimate the maximal reaction rate from the true overall reaction rate, v_{out}.

$$\zeta = \frac{S_{in}}{v_{actual}} \quad \rightarrow \quad S_{in} = v_{max} = \zeta v_{out} \tag{23}$$

Using a bioreactor like device, the system modeled in this study can be replicated by pumping substrate into the system that contains an initial enzyme concentration E_0, at a constant rate, such that at any time, T, $C_S(T) >> C_E(T)$. Then, measuring the rate of product produced,

v_{out}, equation (23) can be used to calculate v_{max}. To this point, the experimental procedure is very similar to that of Michaelis Menten analysis where the rate of reaction is calculated as function of substrate concentration. However, to deduce each individual reaction rate, instead of a lower resolution Michaelis Rate, either the steady state concentration of enzyme or complex must be measured. This crucial piece of information allows for unambiguous definition of rate constants due to the injectivity of equation (13).

In this study, the vast complexity and information that can be deduced from analysis of a simple network demonstrates the importance of quantitative approaches within biological systems. Through careful analysis, mechanisms of regulation can be found within mathematical models, and stable dynamics can be identified. Biological networks are too complex to infer using simplistic modeling, and there is a great need within the scientific community to develop frameworks to interpret and integrate high throughput biological data. However, before actual mechanisms can be discovered through analysis of this data, mechanistic models need to be developed such that the unknown parameters are identified and then approaches can be developed to either estimate these parameters from existing experimental data or protocols can be developed to glean the necessary biological insight. With computation, experimentation, and mathematical analysis operating in parallel, the biochemical networks that control life can be unraveled and modeled such that detailed quantitative predictions are made and emergent phenomena are identified.

References

Érdi, P. (1989). *Mathematical models of chemical reactions : theory and applications of deterministic and stochastic models*: Manchester : Manchester University Press.

Feist, A. M., & Palsson, B. O. (2010). The biomass objective function. *Curr Opin Microbiol, 13*(3), 344-349. doi:10.1016/j.mib.2010.03.003

Gianchandani, E. P., Chavali, A. K., & Papin, J. A. (2010). The application of flux balance analysis in systems biology. *Wiley Interdiscip Rev Syst Biol Med, 2*(3), 372-382. doi:10.1002/wsbm.60

Goudar, C. T., Sonnad, J. R., & Duggleby, R. G. (1999). Parameter estimation using a direct solution of the integrated Michaelis-Menten equation. *Biochim Biophys Acta, 1429*(2), 377-383.

Grima, R., & Schnell, S. (2006). A systematic investigation of the rate laws valid in intracellular environments. *Biophys Chem, 124*(1), 1-10. doi:10.1016/j.bpc.2006.04.019

Gräter, F., & Li, W. (2015). Transition path sampling with quantum/classical mechanics for reaction rates. *Methods Mol Biol, 1215*, 27-45. doi:10.1007/978-1-4939-1465-4_2

Haggart, C. R., Bartell, J. A., Saucerman, J. J., & Papin, J. A. (2011). Whole-genome metabolic network reconstruction and constraint-based modeling. *Methods Enzymol, 500*, 411-433. doi:10.1016/B978-0-12-385118-5.00021-9

Jones, E., Oliphant, E., Peterson, P., & al., e. (2001). SciPy: Open Source Scientific Tools for Python. In: http://www.scipy.org/.

Michaelis, L., Menten, M. L., Johnson, K. A., & Goody, R. S. (2011). The original Michaelis constant: translation of the 1913 Michaelis-Menten paper. *Biochemistry, 50*(39), 8264-8269. doi:10.1021/bi201284u

Schnell, S. (2014). Validity of the Michaelis-Menten equation--steady-state or reactant stationary assumption: that is the question. *FEBS J, 281*(2), 464-472. doi:10.1111/febs.12564

van Der Walt, S., amp, X, Fan, Colbert, S. C., & Varoquaux, G. (2011). The NumPy Array: A Structure for Efficient Numerical Computation. *Computing in Science & Engineering, 13*(2), 22-30. doi:10.1109/MCSE.2011.37

Zhou, H. X., Rivas, G., & Minton, A. P. (2008). Macromolecular crowding and confinement: biochemical, biophysical, and potential physiological consequences. *Annu Rev Biophys, 37*, 375-397. doi:10.1146/annurev.biophys.37.032807.125817